JMEPEG (2010) 19:335–341
DOI: 10.1007/s11665-009-9481-z

1059-9495/$19.00

Using Microwave-Assisted Powder Metallurgy Route and Nano-size Reinforcements to Develop High-Strength Solder Composites

S.M.L. Nai, J.V.M. Kuma, M.E. Alam, X.L. Zhong, P. Babaghorbani, and M. Gupta

(Submitted November 18, 2008; in revised form May 16, 2009)

In the present study, Sn-0.7Cu and Sn-3.5Ag lead-free solders used in the electronics packaging industry were reinforced with different volume percentages of nano-size alumina and tin oxide particulates, respectively, to synthesize two new sets of nanocomposites. These composites were developed using microwave-assisted powder metallurgy route followed by extrusion. The effects of addition of particulates on the physical, microstructural, and mechanical properties of the nanocomposites were investigated. Mechanical properties (microhardness, 0.2% YS, and UTS) for both composite systems increase with the presence of particulates. The best tensile strength was realized for composite solders reinforced with 1.5 vol.% alumina and 0.7 vol.% tin oxide particulates, which far exceeds the strength of eutectic Sn-Pb solder. The morphology of pores was observed to be one of the most dominating factors affecting the strength of materials.

Keywords lead-free solder, metal-matrix nanocomposite, microwave sintering, tensile properties

1. Introduction

For decades, tin-lead (Sn-Pb) solders have been widely utilized in the electronics industry to attach components to printed circuit boards due to their unique properties of low melting point, wetting characteristics, and mechanical properties (Ref 1, 2). However, progressive technological demands in the area of device packaging, environmental concerns, and strict legislations on banning Pb-based solders have created a drive to move beyond such conventional Pb-bearing solders. Lead-free solder is an alternative to address the environmental concerns (Ref 1, 2). Nevertheless, with the miniaturization of integrated circuits, better performance from interconnection joints is essential. A viable way to enhance the performance of a solder is to intentionally incorporate a second phase (such as nano-size reinforcement particulates) into a solder alloy, thus forming a composite solder. The composite approach is proposed as a potential mechanism to improve the service performance of the solder joints. Sn-Cu and Sn-Ag solders are commonly used lead-free solders (Ref 1-3) in place of Sn-Pb solders and are thus selected for investigation in this study.

The processing technique of composite materials also plays a crucial role in the end properties of the materials. The processing routes to fabricate composite solder materials can be broadly classified into the liquid metallurgy and powder metallurgy (PM) routes. The latter is widely used to produce high performance metallic materials for various applications as it offers advantages such as (i) a more refined microstructure, (ii) near-net shape, and (iii) greater utilization of materials. In the PM method, sintering plays a crucial part in realizing the end properties of the materials whereby densification and the formation of bonds (to minimize the level of porosity) take place (Ref 4). Sintering can be performed by the conventional method of heating (such as resistance heating) (Ref 4, 5) or by the more recently introduced sintering approach using microwaves (Ref 6, 7). The direction of resistance heating is from the outside to the inside of the compacted powder preform, and this often results in poor microstructural characteristics of the core of the preform (Ref 5). To circumvent the issues faced by conventional sintering using a resistance heating furnace, a two-directional rapid microwave sintering approach was developed (Ref 8). This microwave sintering approach results in more uniform heating and is also cost-effective and energy efficient.

Recently, solid-state bonding techniques (such as thermal compression and thermosonic and ultrasonic bonding) for solder materials have been introduced (Ref 9-11). Since these techniques do not involve the melting of solder materials (unlike conventional reflow process), the concern of segregation of reinforcement particulates, which could restrict the industrial use of composite solders, will no longer be an issue. The properties of the solder materials fabricated by the PM method can thus be retained when using these solid-state bonding techniques.

The result of a literature search at the start of our research work revealed that no research attempt was made to process solder-related materials using the powder metallurgy technique, particularly adopting energy efficient two-directional microwave sintering process. Accordingly, in this study pure tin

S.M.L. Nai and **J.V.M. Kuma**, Minerals, Metals and Materials Technology Centre, National University of Singapore, 9 Engineering Drive 1, Singapore 117576, Singapore; and **M.E. Alam, X.L. Zhong, P. Babaghorbani,** and **M. Gupta**, Department of Mechanical Engineering, National University of Singapore, 9 Engineering Drive 1, Singapore 117576, Singapore. Contact e-mail: sharonnai9@yahoo.com.

materials were first synthesized using the PM technique using different sintering methodologies (i.e., with two-directional microwave sintering and conventional sintering). The effects of sintering method were investigated. Sn-0.7Cu- and Sn-3.5Ag-based nanocomposites containing nano-size alumina and tin oxide particulates, respectively, were subsequently synthesized using the PM technique. The nanocomposites obtained were characterized for their physical, microstructural, and mechanical properties. Particular emphasis was placed to correlate the effect of increasing volume percent of reinforcement particulates with the physical, microstructural, and mechanical properties of the nanocomposites obtained.

2. Experimental Procedures

2.1 Materials

In this study, three different materials were used as matrix material. They are (i) pure tin powder with −325 mesh size (less than 44 μm) of 99.9% purity (supplied by NOAH Technologies Corporation, Texas, USA), (ii) Sn-0.7Cu solder powder with size range of 20 to 38 μm (supplied by Qualitek®, USA), and (iii) Sn-3.5Ag powder with a size range of 25 to 45 μm (supplied by Qualitek®, USA). Two reinforcements were used, namely, (i) SnO_2 nanopowder with a size range of 60 to 80 nm (supplied by NanoAmor, USA) and (ii) Al_2O_3 nanopowder with average size of 50 nm (supplied by Advanced Pinnacle Technologies, Singapore).

2.2 Processing of Monolithic Materials and Nanocomposites

2.2.1 Pure Sn Materials. Preweighed pure Sn powder was uniaxially compacted using a pressure of 510 MPa to billets (40 mm height with 35 mm diameter). Compacted billets were then sintered using rapid microwave-assisted sintering technique to reach the temperature of 226 °C under ambient condition in a 900 W, 2.45 GHz SHARP microwave oven. SiC is used as the microwave susceptor material. SiC powder (contained within a microwave-transparent ceramic crucible) absorbs microwave energy readily at room temperature and is heated quickly, providing the radiant heat to heat the billet externally while the compacted billet absorbs microwaves and is heated from within. The set time only included heating time, and there was no holding time to minimize or eliminate bulk and/or localized melting of samples. This hybrid heating method results in a more uniform temperature gradient within the billet and circumvents the disadvantages of heating using either conventional heating or microwaves alone. In order to compare the results with that of radiant heat sintering, Sn billets processed in an identical way were conventionally sintered at 156 °C ($0.85T_m$) for 2 h in a tube furnace under Argon atmosphere. The sintered billets were hot extruded at 230 °C into 7 mm diameter rods. The billets were first soaked at 230 °C for 5 min in a constant temperature furnace before extrusion (Ref 12, 13).

2.2.2 Monolithic Sn-3.5Ag and Sn-3.5Ag/SnO_2 Nanocomposites. Sn-3.5Ag powder and SnO_2 nanopowder were weighed and mixed homogeneously in a RETSCH PM-400 mechanical alloying machine using a speed of 200 rpm for 1 h. No balls or process control agent was used during blending step. The blended mixtures were compacted and then sintered using microwave-assisted sintering technique to reach the temperature of 221 °C. The sintered billets were subsequently hot extruded at 221 °C to produce an extruded rod with a final diameter of 7 mm. The billets were also soaked at 221 °C for 5 min in a constant temperature furnace before extrusion. Monolithic Sn-3.5Ag billet was fabricated directly by compaction and sintering, thereby omitting the mixing process (Ref 14).

2.2.3 Monolithic Sn-0.7Cu and Sn-0.7Cu/Al_2O_3 Nanocomposites. Sn-0.7Cu powder and Al_2O_3 nanopowder were weighed and mixed in a V-blender. The blended mixtures were compacted and then sintered using microwave-assisted sintering technique to reach the temperature of 210 °C. The sintered compacts were subsequently extruded at room temperature into 7 mm diameter rods. Monolithic Sn-0.7Cu samples were processed using the same parameters (omitting the mixing process) as the nanocomposites for comparison purposes (Ref 15, 16).

2.3 Characterization Studies

Density of polished extruded solder materials was determined using Archimedes' principle (Ref 17). Distilled water was used as immersion fluid.

Microstructural analysis of the metallographically polished samples of the solder materials was carried out using JEOL JSM 5800 LV Scanning Electron Microscope (SEM) equipped with Energy Dispersive Spectroscopy (EDS) and HITACHI Field Emission Scanning Electron Microscopy (FE-SEM). Image analysis using the Scion system was carried out to quantify the microstructural features.

Microhardness measurements were performed on the polished monolithic and nanocomposite samples using a Matsuzawa MXT 50 automatic digital microhardness tester. Microhardness tests were performed using a Vickers indenter in accordance with the ASTM standard E384-99.

The tensile properties of the extruded samples were determined in accordance with ASTM test method E8M-01. The tensile tests were conducted on round tension test samples of diameter 5 mm and gauge length 25 mm, using an automated servohydraulic testing machine (MTS 810) with a crosshead speed set at 0.254 mm/min. Tests were performed at ambient temperature. The 0.2% yield strength (0.2% YS), ultimate tensile strength (UTS), and failure strain (FS) values of the materials were determined by plotting the respective stress-strain curves.

3. Results

3.1 Density Measurement

The results of density measurement of the respective extruded solder samples are shown in Table 1. The results revealed that microwave-sintered pure Sn samples had higher density than those conventionally sintered. The density of Sn-0.7Cu nanocomposites decreased with increasing presence of Al_2O_3 particulates. In the case of Sn-3.5Ag-based samples, the density values are statistically the same, except with the addition of 1.0 vol.% of SnO_2 particulates.

3.2 Microstructure Characterization

Microstructural studies were conducted on the extruded samples to investigate: (i) the distribution of nano-size

reinforcements, (ii) the presence and distribution of intermetallic compounds (IMCs), (iii) the presence and morphology of pores, and (iv) the interface characteristics between solder and reinforcement. Microwave-sintered pure Sn samples showed lower porosity level and pores aspect ratio, as compared with those conventionally sintered (see Table 2). In the case of Sn-0.7Cu-based nanocomposites, porosity level and pores aspect ratio were observed to increase with increasing amount of Al_2O_3 particulates. However, in the case of Sn-3.5Ag-based nanocomposites, porosity level was observed to be statistically unchanged with increasing amount of SnO_2 particulates. Furthermore, when the amount of SnO_2 was increased from 0.7 to 1 vol.%, a significant increase in pores aspect ratio was observed (see Table 2). Representative micrographs showing the pores morphology of monolithic Sn-3.5Ag and Sn-3.5Ag/SnO_2 nancomposites are shown in Fig. 1.

For Sn-0.7Cu/Al_2O_3 and Sn-3.5Ag/SnO_2 nanocomposites, the investigation conducted using FE-SEM revealed the

Table 1 Results of density and porosity

Materials	Amount of reinforcement, vol.%	Density, g/cm^3
Sn-MW	…	7.252 ± 0.031
Sn-CS	…	7.230 ± 0.007
Sn-0.7Cu	…	7.269 ± 0.014
Sn-0.7Cu/0.5%Al_2O_3	0.5	7.234 ± 0.023
Sn-0.7Cu/1.5%Al_2O_3	1.5	7.126 ± 0.066
Sn-3.5Ag	…	7.316 ± 0.006
Sn-3.5Ag/0.7%SnO_2	0.7	7.312 ± 0.009
Sn-3.5Ag/1.0%SnO_2	1.0	7.286 ± 0.009

MW: microwave-assisted sintering; CS: conventional sintering

Table 2 Results of porosity level and pores aspect ratio

Materials	Porosity, %	Pores aspect ratio (a)
Sn-MW	0.6 ± 0.4 (b)	1.5 ± 0.5
Sn-CS	0.9 ± 0.1 (b)	3.4 ± 1.3
Sn-0.7Cu	0.51 (b)	1.3
Sn-0.7Cu/0.5%Al_2O_3	0.77 (b)	1.6
Sn-0.7Cu/1.5%Al_2O_3	1.80 (b)	1.9
Sn-3.5Ag	0.6 ± 0.05 (c)	1.3 ± 0.24
Sn-3.5Ag/0.7%SnO_2	0.6 ± 0.20 (c)	1.6 ± 0.32
Sn-3.5Ag/1.0%SnO_2	0.9 ± 0.12 (c)	2.7 ± 0.34

(a) At least 50 pores were quantified in each case
(b) Porosity level was calculated by comparing the experimental and theoretical densities
(c) Scion Image software was used to determine the porosity level

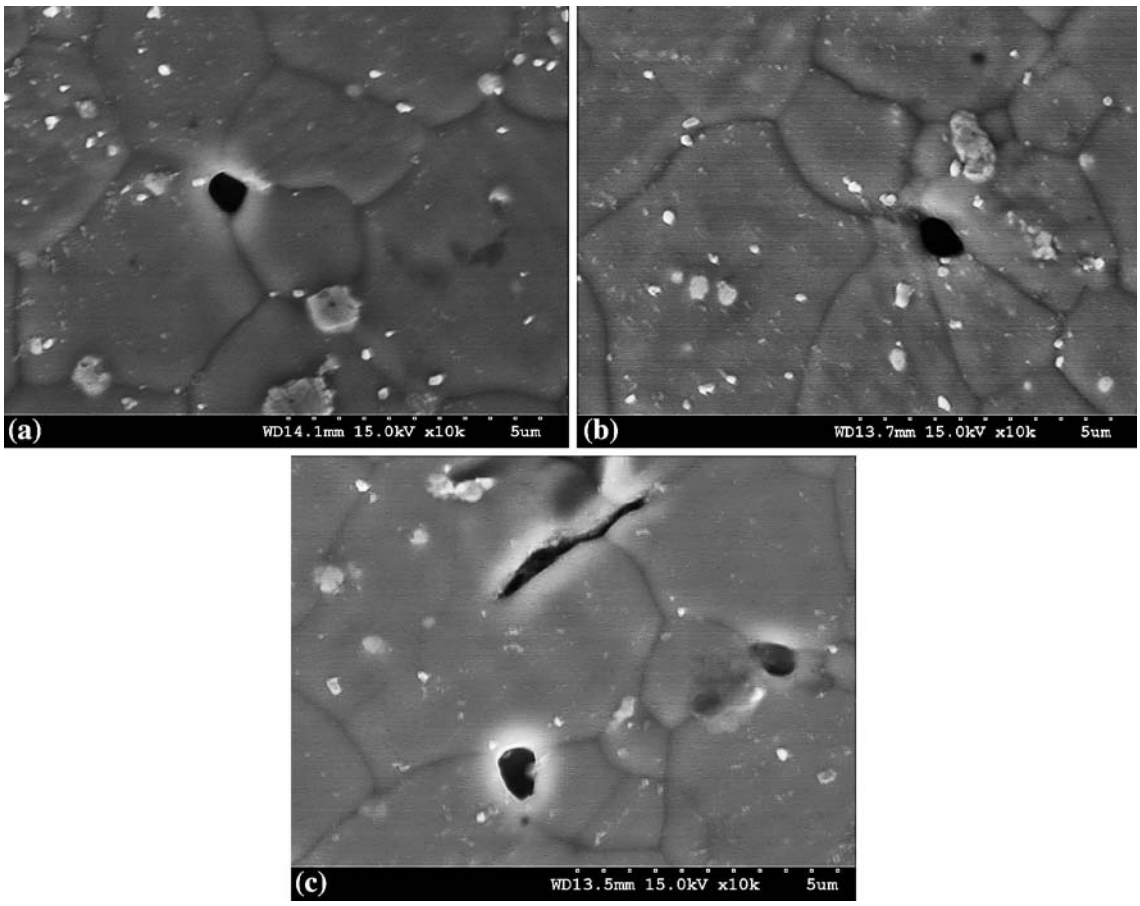

Fig. 1 Representative FE-SEM micrographs showing pores morphology of: (a) Sn-3.5Ag, (b) Sn-3.5Ag/0.7% SnO_2, and (c) Sn-3.5Ag/1.0%SnO_2

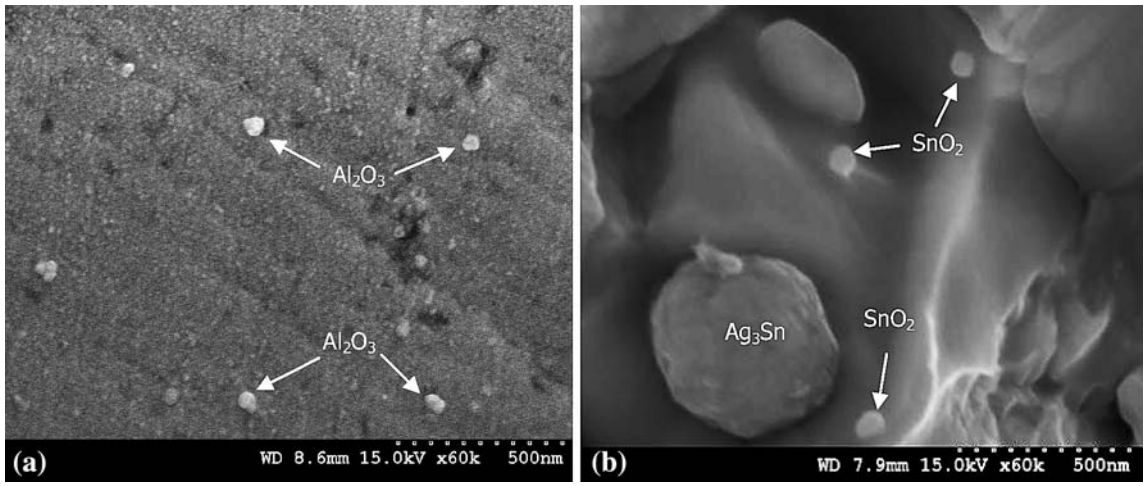

Fig. 2 Representative FE-SEM micrographs showing the presence of nano-size: (a) Al_2O_3 particulates in Sn-0.7Cu/Al_2O_3 composite solder and (b) SnO_2 particulates in Sn-3.5Ag/SnO_2 composite solder

presence and a fairly uniform distribution of reinforcement particulates (see Fig. 2). Good interfacial integrity was also observed between the solder matrix and reinforcement (see Fig. 2). There was no void between the reinforcement and solder matrix. For monolithic Sn-0.7Cu and Sn-0.7Cu/Al_2O_3 composites, intermetallic compounds were also uniformly distributed in the solder matrix. The EDS analysis (see Fig. 3) revealed the presence of Sn and Cu phases and the intermetallic compound was identified to be the Cu_6Sn_5 phase. Similarly, for monolithic Sn-3.5Ag and Sn-3.5Ag/SnO_2 composites, intermetallic compounds were uniformly distributed in the solder matrix. The EDS analysis (see Fig. 3) revealed the presence of Sn and Ag phases and the intermetallic compound was identified to be the Ag_3Sn phase.

3.3 Mechanical Behavior

The mechanical behavior of the extruded samples was assessed in terms of their microhardness and tensile properties (see Table 3).

For Sn-0.7Cu/Al_2O_3 and Sn-3.5Ag/SnO_2 samples, microhardness values increased marginally with increasing amount of respective reinforcement particulates.

Tensile tests at ambient temperature revealed better combination of tensile properties (30% higher YS, 26% higher UTS, and 12% higher FS) for microwave-sintered pure Sn samples than those conventionally sintered. For Sn-0.7Cu/Al_2O_3 composites, a significant improvement in 0.2% YS (up to ~135%) and UTS (up to ~135%) was observed with increasing vol.% of nano-size Al_2O_3 particulates. However, FS showed a decreasing trend with increasing amount of reinforcement.

For Sn-3.5Ag/SnO_2 composites, tensile results revealed that strength improvement of Sn-3.5Ag matrix can be realized when the amount of SnO_2 increased to 0.7 vol.%. Sn-3.5Ag/0.7%SnO_2 samples showed 18 and 31% higher 0.2% YS and UTS, respectively, over monolithic samples. The increase is more significant (~98% higher YS and ~118% higher UTS) when compared with the Sn-3.5Ag value provided by Qualitek® (see Table 3). It was also noted that though FS decreased with increasing amount of SnO_2 particulates, the FS values of the nanocomposites were still better, if not comparable with the FS value provided by Qualitek®.

4. Discussion

4.1 Pure Sn Materials

Significant energy savings can be achieved using microwave heating as microwave energy is transferred directly to the solder material, in contrast to conventional heating whereby energy is expended in heating the resistive coils, surrounding atmosphere, and the inner walls of the tube furnace. The two-directional microwave sintering approach used in this study results in a significant energy savings of more than 90% when compared with the conventional sintering approach (Ref 18). This will definitely be economically viable for industries and environmentally friendly in terms of lower CO_2 emission.

Better densification obtained in microwave-sintered pure Sn samples can be attributed to the higher sintering temperature which resulted in faster migration of atoms in accordance with the fundamental principles of diffusion (Ref 4, 5, 19). This is despite the fact that no holding time was given during the microwave sintering in this study. Moreover, higher aspect ratio of the pores in the case of conventionally sintered samples suggested that intermediate stage of sintering was achieved even when the holding duration was 2 h. In the case of microwave sintered samples, the absence of lenticular pores indicated that a rapid sintering duration (~7 min) in microwaves can bring the sintering into its final stage (Ref 4).

In this study, it was observed that the morphology of pores played a dominating role in influencing the tensile properties of the materials. The lower strength values in conventionally sintered samples could be due to the pore morphology, where the sharp edge pores present act as stress concentration sites, leading to premature failure. This observation is consistent with the findings of other investigators working on Al- and Mg-based materials (Ref 7, 8) who similarly reported that pore morphology was more instrumental in enhancing tensile strength. More detailed explanation of this study is presented in Ref 12 and 13.

4.2 Sn-3.5Ag/SnO_2 and Sn-0.7Cu/Al_2O_3 Nanocomposites

Microstructural studies revealed fairly uniform distribution of SnO_2 and Al_2O_3 reinforcement particulates in their

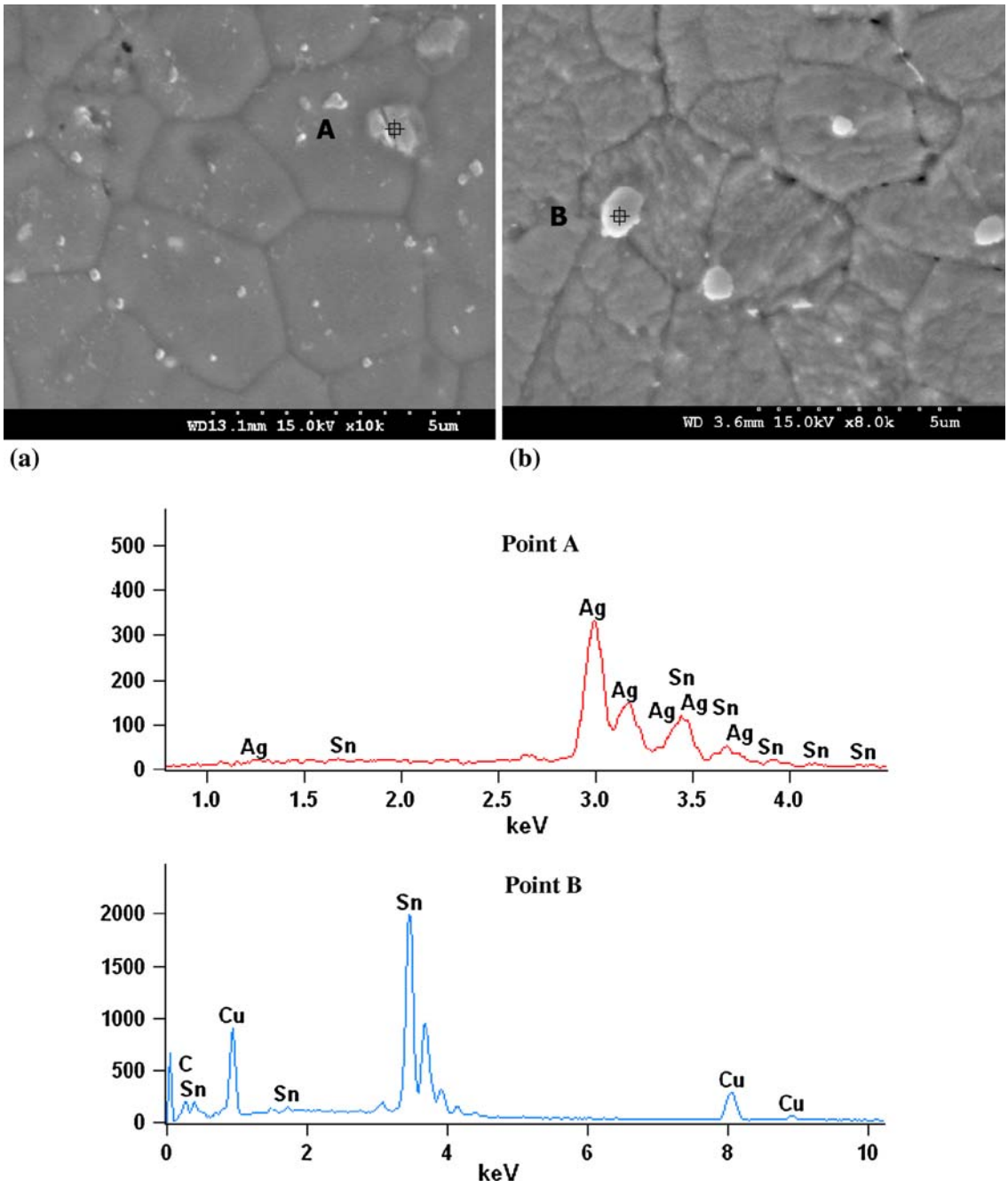

Fig. 3 Representative FE-SEM micrographs showing the presence of intermetallic compounds in the solder matrix and EDS analysis showing the presence of phases in: (a) monolithic Sn-3.5Ag and Sn-3.5Ag/SnO_2 composite solder and (b) monolithic Sn-0.7Cu and Sn-0.7Cu/Al_2O_3 composite solder

respective solder matrices. Theoretically, when secondary process with a large enough deformation is introduced, homogenous distribution of reinforcement can be achieved regardless of the size difference between matrix powder and reinforcement particulates (Ref 20). Hence, the reasonably uniform distribution of reinforcement particulates observed in this study confirms the efficiency of blending and extrusion parameters used. It may be noted that one of the essential factor for the extent of strengthening that can be realized in composite materials is the uniform distribution of reinforcement particulates in the matrix (Ref 21-24).

The increase in average microhardness due to the presence of nano-size reinforcement particulates can be attributed primarily to: (i) the presence of harder reinforcement particulates and (ii) higher constraint to the localized matrix deformation during indentation as a result of the presence of reinforcement particulates. The presence of stronger and stiffer particulates assist in obstructing localized plastic deformation of the solder matrix during microhardness indentation. Furthermore, the large difference in CTE between solder alloy matrix and reinforcement particulates leads to higher dislocation density in the matrix and this resulted in the hardening of

Table 3 Results of tensile properties of solder materials

Materials	Microhardness, HV	0.2% YS, MPa	UTS, MPa	FS, %
Sn-MW	…	35 ± 2	39 ± 3	10.0 ± 0.5
Sn-CS	…	27 ± 5	31 ± 5	8.9 ± 0.8
Sn-0.7Cu	8.8 ± 0.2	17 ± 1	20 ± 1	33.6 ± 3.0
Sn-0.7Cu/0.5%Al_2O_3	9.3 ± 0.2	29 ± 4	32 ± 3	14.7 ± 0.1
Sn-0.7Cu/1.5%Al_2O_3	10.3 ± 0.3	40 ± 1	47 ± 1	10.0 ± 0.2
Sn-3.5Ag	14 ± 1	38 ± 1	44 ± 0	45.7 ± 0.6
Sn-3.5Ag/0.7%SnO_2	17 ± 1	45 ± 1	58 ± 2	24.0 ± 0.5
Sn-3.5Ag/1.0%SnO_2	17 ± 1	40 ± 4	44 ± 5	20.8 ± 0.5
Sn-0.7Cu (a)	…	15	22	39
Sn-3.5Ag (a)	…	22	27	24
Sn-37Pb (a)	…	27	31	48

YS: yield strength; UTS: ultimate tensile strength; FS: failure strain
(a) Company catalog provided by Qualitek®, USA, 2006

the matrix. The results obtained in this study are consistent with the observations made in earlier studies (Ref 25).

The improvement in nanocomposite strength over their monolithic counterparts can be attributed to: (i) Orowan strengthening mechanism due to the presence of nano-size reinforcement particulates in the solder matrix (Ref 26-29), (ii) increase in dislocation density due to coefficient of thermal expansion (CTE) mismatch between solder alloy matrices and their respective reinforcement particulates (Ref 30, 31), (iii) elastic modulus mismatch between matrix and reinforcement (Ref 32), (iv) effective load transfer due to the presence of reinforcements and good interfacial bonding between the matrix and reinforcement (Ref 33), and (v) the presence of more near-equiaxed pores in the material.

However, it was noted that there is a decline in material strength (Sn-3.5Ag/1.0%SnO_2) when the amount of SnO_2 increased from 0.7 to 1.0 vol.%. This can be due to the higher porosity level (~0.9%) as well as higher pores aspect ratio (~2.7) (see Table 2). The higher pores aspect ratio in Sn-3.5Ag/1.0%SnO_2 signified the presence of sharp edge pores in the microstructure (see Fig. 1c) which justified the lower tensile properties in this material. Porosity serves as a crack initiation site and its adverse effects on the material strength has been established convincingly for both monolithic and composite materials (Ref 34, 35). It has also been reported by others that a threshold exists whereby incorporation of too much reinforcement could lead to detrimental effect on the material properties (Ref 35, 36). In comparison with the widely used Sn-37Pb solder (see Table 3), the nanocomposites synthesized in this study exhibited an overall improvement in 0.2% YS and UTS.

The failure strain of all nanocomposite samples exhibited a decreasing trend with increasing amount of reinforcement particulates (see Table 3). This can be attributed to: (i) the corresponding increasing porosity level (see Table 2) and (ii) the presence of harder reinforcing phase, which serves as crack nucleation sites, leading to a decrease in FS under tensile loading conditions (Ref 24, 37, 38). More discussion on Sn-3.5Ag/SnO_2 and Sn-0.7Cu/Al_2O_3 nanocomposites is detailed in Ref 14-16.

5. Conclusions

(1) Powder metallurgy route coupled with sintering and extrusion was used to successfully synthesize monolithic (Sn, Sn-3.5Ag, and Sn-0.7Cu) and nanocomposite (Sn-3.5Ag/SnO_2 and Sn-0.7Cu/Al_2O_3) solder materials.

(2) Microwave-sintered pure Sn samples exhibited superior microstructural features (in terms of lower porosity level and near-equiaxed pores aspect ratio) and better mechanical properties (in terms of higher 0.2% YS, UTS, and FS) when compared to conventionally sintered samples.

(3) Microstructural characterization of the nanocomposite samples (Sn-3.5Ag/SnO_2 and Sn-0.7Cu/Al_2O_3) revealed that intermetallic compounds and nano-size reinforcement particulates were uniformly dispersed throughout the respective matrices.

(4) The best overall combination of mechanical properties was achieved in Sn-3.5Ag reinforced with 0.7 vol.% SnO_2 particulates and Sn-0.7Cu reinforced with 1.5 vol.% Al_2O_3 particulates.

(5) The morphology of pores was observed to be one of the most dominating factors affecting the strength of the materials.

Acknowledgments

The authors acknowledge the support received for this research work ref: C-534-000-003-414 from the Minerals, Metals and Materials Technology Centre (M3TC) of the National University of Singapore.

References

1. P.T. Vianco, *Handbook of Lead-free Solder Technology for Microelectronic Assemblies*, Marcel Dekker, Inc., New York, 2004, p 167–210
2. M. Abtew and D. Selvaduray, Lead-free Solders in Microelectronics, *Mater. Sci. Eng. R: Rep.*, 2000, **27**(5–6), p 95–141
3. European Lead-free Soldering Network, Lead-free Soldering Status Survey 2006. http://www.europeanleadfree.net. Assessed on 10 April 2008
4. R.M. German, *Sintering Theory and Practice*, John Wiley and Sons Inc., New York, 1996
5. J.P. Schaffer, A. Saxena, S.D. Antolovich, T.H. Sanders, and S.B. Warner, *The Science and Design of Engineering Materials*, McGraw-Hill, New York, 1999
6. J. Cheng, D.K. Agrawal, S. Komaneni, M. Mattis, and R. Roy, Microwave Processing of WC-Co Composites and Ferroic Titanates, *Mater. Res. Innov.*, 1997, **1**, p 44–52
7. R.M. Anklekar, D.K. Agrawal, and R. Roy, Microwave Sintering and Mechanical Properties of PM Copper Steel, *Powder Metall.*, 2001, **44**, p 355–362
8. M. Gupta and W.L.E. Wong, Overall Mechanical Performance of Metallic Materials Using Two-Directional Microwave Assisted Rapid Sintering, *Scripta Mater.*, 2005, **52**, p 479–483
9. J.M. Kim, J.P. Jung, Y.N. Zhou, and J.Y. Kim, Ambient Temperature Ultrasonic Bonding of Si-dice Using Sn-3.5 wt.%Ag, *J. Electron. Mater.*, 2008, **37**(3), p 324–330
10. Y. Tomita, M. Tago, Y. Nemoto, and K. Takahashi, *Electronic Mater. Pack., EMAP 2001*, 19–22 Nov 2001, p 107
11. P.H. Lawyer, D. Choudhury, M.D. Wetzel, and D.B. Rensch, *Electro. Manuf. Tech. Sym. 23rd IEEE/CPMT*, 19–21 Oct 1998, p 390
12. M.E. Alam and M. Gutpa, Effects of Sintering and Its Type on Microstructural and Tensile Response of Pure Tin, *Powder Metall.*, 2008. doi:10.1179/174329008X 284895
13. M.E. Alam and M. Gupta, Tensile Behavior of Tin Sintered Using Microwaves and Radiant Heating, *Proceedings of ICME 2007*, ICME07-AM-15, 29–31 Dec 2007, Dhaka, Bangladesh, 2007
14. P. Babaghorbani, S.M.L. Nai, and M. Gupta, Development of Lead-free Nanocomposite Solders Using Oxide Based Reinforcement, *Proceedings of ASME IMECE 2008*, 31 Oct-6 Nov 2008, Boston, USA, 2008

15. X.L. Zhong and M. Gupta, Development of Lead-free Sn-0.7Cu/Al_2O_3 Nanocomposite Solders with Superior Strength, *J. Phys. D: Appl. Phys.*, 2008, **41**, p 095403
16. X.L. Zhong and M. Gupta, Synthesis and Characterization of Lead-free Solder/Nano-Alumina Composites, *Proceedings in Processing and Fabrication of Advanced Materials (PFAM XVI) 2007*, 17–19 Dec 2007, p 186–195
17. M. Gupta, M.O. Lai, and D. Saravanaranganathan, Synthesis, Microstructure and Properties Characterization of Disintegrated Melt Deposited Mg/SiC Composites, *J. Mater. Sci.*, 2000, **35**, p 2155–2165
18. W.L.E. Wong and M. Gupta, Improving Overall Mechanical Performance of Magnesium Using Nano-Alumina Reinforcement and Energy Efficient Microwave Assisted Processing Route, *Adv. Eng. Mater.*, 2007, **9**(10), p 902–909
19. R.M. German, *Powder Metallurgy Science, Metal Powder Industries Federation*, Princeton, NJ, 1994, p 261–264
20. M.J. Tan and X. Zhang, Powder Metal Matrix Composites: Selection and Processing, *Mater. Sci. Eng. A*, 1998, **244**, p 80–85
21. H. Mavoori and S. Jin, New, Creep-Resistant, Low Melting Point Solders with Ultrafine Oxide Dispersions, *J. Electron. Mater.*, 1998, **27**, p 1216–1222
22. X.L. Zhong and M. Gupta, High Strength Lead-free Composite Solder Materials Using Nano-Al_2O_3 as Reinforcement, *Adv. Eng. Mater.*, 2005, **7**(11), p 1049–1054
23. S.M.L. Nai, J. Wei, and M. Gupta, Development of Advanced Lead-free Solder Based Interconnect Materials Containing Nanosized Y_2O_3 Particulates, *Proceedings of ASME IMECE 2005*, 5–11 Nov 2005, Orlando, USA, 2005
24. S.M.L. Nai, J. Wei, and M. Gupta, Development of Lead-free Solder Composites Containing Nanosized Hybrid (ZrO_2 + 8 mol.% Y_2O_3) Particulates, *Solid State Phenom.*, 2006, **111**, p 59–62
25. D.J. Lloyd, Particle Reinforced Aluminium and Magnesium Matrix Composites, *Int. Mater. Rev.*, 1994, **39**(1), p 1–23
26. I. Shao, P.M. Verrcken, C.L. Chien, P.C. Searson, and R.C. Cammarata, Synthesis and Characterization of Particle-Reinforced Ni/Al_2O_3 Nanocomposites, *J. Mater. Res.*, 2002, **17**, p 1412–1418
27. L. Thilly, M. Véron, O. Ludwig, and F. Lecouturier, Deformation Mechanism in High Strength Cu/Nb Nanocomposites, *Mater. Sci. Eng. A*, 2001, **309**, p 510–513
28. G.E. Dieter, *Mechanical Metallurgy*, McGraw-Hill, Inc., USA, 1976, p 191–193
29. Q. Zhang and D.L. Chen, A Model for Predicting the Particle Size Dependence of the Low Cycle Fatigue Life in Discontinuously Reinforced MMCs, *Scripta Mater.*, 2004, **51**, p 863–867
30. N. Hansen, The Effect of Grain Size and Strain on the Tensile Flow Stress of Aluminium at Room Temperature, *Acta Metall.*, 1977, **25**(8), p 863–869
31. D.C. Dunand and A. Mortensen, On plastic Relaxation of Thermal Stresses in Reinforced Metals, *Acta Metall. Mater.*, 1991, **39**(2), p 127–139
32. Z. Száraz, Z. Trojanová, M. Cabbibo, and E. Evangelista, Strengthening in a WE54 Magnesium Alloy Containing SiC Particles, *Mater. Sci. Eng. A*, 2007, **462**, p 225–229
33. N. Ramakrishnan, An Analytical Study on Strengthening of Particulate Reinforced Metal Matrix Composites, *Acta Mater.*, 1996, **44**(1), p 69–77
34. C. Tekmen, I. Ozdemir, Ü. Cöcen, and K. Önel, The Mechanical Response of Al-Si-Mg/SiCp Composite: Influence of Porosity, *Mater. Sci. Eng. A*, 2003, **360**, p 365–371
35. S.M.L. Nai, J. Wei, and M. Gupta, Lead-free Solder Reinforced with Multi-Walled Carbon Nanotubes, *J. Electron. Mater.*, 2006, **35**(7), p 1518–1522
36. L. Wang, D.Q. Yu, S.Q. Han, H.T. Ma, and H.P. Xie, The Evaluation of the New Composite Lead Free Solders with the Novel Fabricating Process, *Int'l. Conference on the Business of Electron. Product Reliability and Liability*, 2004, p 50–56
37. S. Ugandhar, N. Srikanth, M. Gupta, and S.K. Sinha, Enhancing the Properties of Magnesium Using SiC Particulates in Sub-Micron Length Scale, *Adv. Eng. Mater.*, 2003, **6**(12), p 957–964
38. K.S. Tun and M. Gupta, Improving Mechanical Properties of Magnesium using Nano-Yttria Reinforcement and Microwave Assisted Powder Metallurgy Method, *Compos. Sci. Technol.*, 2007, **67**(13), p 2657–2664